Further improvements in Er^{3+} coupled to Si nanoclusters rib waveguides

A. Pitanti[1], D. Navarro-Urrios[1], R. Guider,[1] N. Daldosso[1], F. Gourbilleau[2], L. Khomenkova[2], R. Rizk[2], and L. Pavesi[1]

[1]Laboratorio di Nanoscienze, Dipartimento di Fisica, Università di Trento, Via Sommarive 14, I-38050 Povo (Trento), Italy
[2]SIFCOM, UMR CNRS 6176, ENSICAEN, 6 Boulevard Maréchal Juin, 14050 CAEN, France

ABSTRACT

The use of broadband efficient sensitizers for Er^{3+} ions relaxes the expensive conditions needed for the pump source and raises the performances of the optical amplifier. Within this context Si nanoclusters (Si-nc) in silica matrices have revealed as optimum sensitizers and open the route towards electrically pumped optical amplifiers. Up to date two have been the main limiting issues for achieving absolute optical gain, the first one is the low quantity of erbium efficiently coupled to the Si-nc while the second is the carrier absorption mechanism (CA) within the Si-nc, which generates additional losses instead of providing amplification.

In this work we will present a detailed study of the optical properties of a set of samples prepared by confocal reactive magnetron co-sputtering of pure SiO_2 and Er_2O_3 targets. The material has been optimised in terms of the increasing of Er^{3+}-related PL intensity and lifetime as well as the decreasing down to 3 dB/cm of the propagation losses in the rib-loaded waveguides outside the absorption peak of erbium. Our signal enhancement results show that we have been able to reduce the CA losses to less than 0.2 dB/cm at pump fluxes as high as 10^{20} ph/cm^2 s. Around 25% of the optically active erbium population has been inverted through indirect excitation (pumping with a 476nm laser line), leading to internal gain coefficients of more than 1 dB/cm.

Keywords: optical amplifier, gain, erbium, silicon nanoclusters, sensitizers

1. INTRODUCTION

Nowadays, Erbium plays a fundamental role in telecomunication technology [1]. The emission peak of Er^{3+} ions falls in the third Telecom Window and this makes them perfect candidates for Fiber Optical Amplification devices. Even if Erbium Doped Silica Fiber Amplifiers (EDFA) represent a well estabilished technology, there is still room for improvement, on one hand by reducing the cost of the expensive lasers needed to pump the sharp, low absorbing (σ_{abs}(@1535nm) ~ 5 x 10^{-21} cm^2) Er transitions [2], and on the other by improving the packaging. The inclusion of broad-band high-absorbing sensitizers as Si nanocrystals/nanoclusters (Si-nc) seems a promising route to realize an Erbium Doped Waveguide Amplifier (EDWA) where the pump laser can be substituted by an high power LEDs or, even, by an electrical excitation circuit [3].

The main obstacles to achieve net optical amplification in Si-nc based EDWA are currently represented by Carrier Absorption (CA) phenomena [4] and by the low number of Er ions efficiently coupled to Si-nc. If the reasons for this low number of coupled ions are still under discussion and different approaches are experienced to overcome this limitation [5], [6], the CA mechanism is a well known phenomenon for bulk semiconductor (Free Carrier Absorption - FCA) [7], but still under study for nano-sized crystals. In a previous work, we have quantified the CA losses in a Si-nc multi-layer sample without Er [4], measuring a maximum loss of 2 cm^{-1} at 1535nm at high pump photon fluxes (~ 10^{20} ph/cm^{2}s).

Recently we have focused on eliminating the CA issue in SRSO Er-doped silica systems. The CA induced losses are proportional to the exciton population density in Si-nc; thus to reduce the CA a faster exciton recombination in small

nanocrystals and/or a faster free carrier population depletion (due, for example, to a transfer mechanism) is needed. In order to realize this we have performed an intensive sample optimization to achieve a high photoluminescence signal together with a long Er ions photoluminescence (PL) lifetime, maintaining a low Si excess in the sample. With an oppportune engineering of Si-nc and increasing the number of Er ions efficiently coupled to Si-nc, we will show a system with negligible CA losses (less than 0.2 dB/cm at 1535nm). Despite this positive result, the percentage of Er ions coupled to the nanocluster should still to be improved in order to obtain net optical amplification in the EDWA.

2. EXPERIMENTAL AND SAMPLE OPTIMIZATION

The layers investigated have been fabricated using an original approach of RF reactive magnetron sputtering of 2-inches confocal pure SiO_2 and Er_2O_3 targets under argon-hydrogen mixture. The ability of the reactive H_2 gas to reduce the oxygen-silicon species originating from the sputtered target was used to modify the incorporation of Si excess in the layers, as previously described [8]. The deposition was performed onto 2-inches silicon substrates covered by stoichiometric thermal silica of 5-μm thickness. More details on sample preparation can be found elsewhere[8]. In this work we will examine a series of samples optimized in terms of high PL emission from Er ions and long Er lifetime for the $4I_{13/2} \rightarrow 4I_{15/2}$ transition (some milliseconds). The optimization of PL properties of the layers has been done as a function of the main deposition parameters, among them: (i) RF power on each cathode, (ii) substrate temperature, T_S, and (iii) hydrogen rate r_H ($r_H = \frac{P_{H_2}}{P_{H_2} + P_{Ar}}$), where P_{H_2} and P_{Ar} are the partial pressure of hydrogen and argon, respectively.

During all deposition runs the applied RF powers on SiO_2 and Er_2O_3 cathodes were 150 W and 15 W, respectively. The total pressure $P_{H_2} + P_{Ar}$ was fixed at 3 mTorr while the r_H value was varied in the range of 20-80%. The effect of T_S on PL properties of deposited layers has been studied by varying T_S from 50°C to 300°.

After the deposition, the layers were annealed at 910 °C during 60 min in nitrogen flow (20 sccm). PL properties were studied at room temperature under excitation by Ar laser with 476nm and 488nm lines with photon flux of $4 \cdot 10^{18}$ ph/cm^2·s. To compare different samples all PL spectra were normalized to the thickness of the active layers.

The optimized samples were then characterized in terms of active layer refractive index and thickness by m-line measurement with visible (543, 633 nm) and infrared (1319, 1542 nm) laser sources [9]. After a top-cladding silica deposition, the slab waveguide has been dry etched to create the channel structure. The etching depth and the channel widths have been chosen in order to optimize the Confinement Factor Γ of the guided mode and to realize a mono-modal optical waveguide.

Table 1 summarizes some of the material and optical characteristics of the samples under study. Samples A and B are the best optimized samples in terms of lifetime and PL, as will be discussed briefly in the following (2.1), while the sample O is the best sample of a previous sample run (annealed under the same conditions) and is therefore used as a reference sample. More information on this sample can be found in [5].

Table 1. Sample A, B and O material and optical characteristics.

Sample label	Si excess [at%]	Er concentration [ions/cm^3]	Thickness [μm]	Lifetime ($4I_{13/2} \rightarrow 4I_{15/2}$) [ms]
A	5 ± 2	3.4 ± 0.2 x 10^{20}	1.2	5.7 ± 0.5
B	8.5 ± 2	3.8 ± 0.4 x 10^{20}	1	5.5 ± 0.5
O	8.5 ± 2	4 ± 0.4 x 10^{20}	1	2.2 ± 0.5

2.1The effect of deposition conditions

The variation of the deposition parameters have been done aiming at optimizing the Er:SRSO layers in terms of efficient PL and long PL lifetime for the $^4I_{13/2} \rightarrow ^4I_{15/2}$ transition of Er^{3+} ions.

After some deposition checks, the applied RF power on SiO_2 and Er_2O_3 cathodes was chosen to be 150 W and 15 W, respectively. The effect of the temperature of substrate, T_S, and of the hydrogen rate r_H on the PL properties was studied, keeping constant all the other deposition and annealing parameters. In particular, Fig. 1 shows the effect of the substrate temperature for a fixed hydrogen rate. PL emission shows a maximum at about 80-100 °C with a rapid decreasing with the increase of T_S, while a gradual decrease of Er^{3+} lifetime from 4.5 ms to 3.0 ms was observed (not shown).

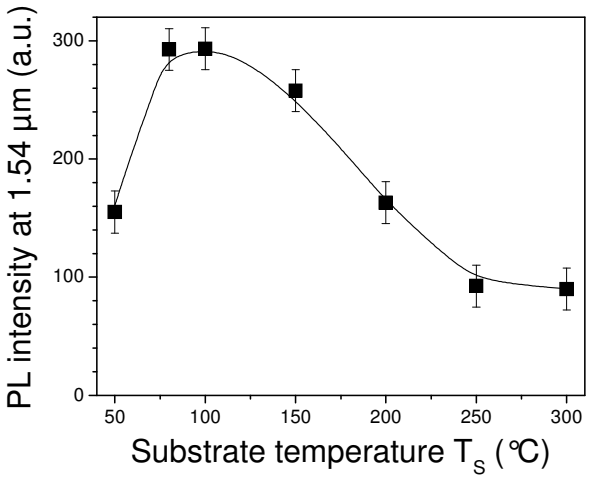

Figure 1. Dependence of Er^{3+} PL intensity of SRSO-Er layers on the temperature of substrate. Deposition conditions: r_H =60 %, P_{SiO2}=150 W, P_{Er2O3}=15 W. PL emission was studied under non-resonant excitation (476nm, photon flux $4 \cdot 10^{18}$ ph/cm^2·s).

To study the effect of the r_H , T_s has been fixed at 100°C. The increase of r_H from 20% to 80% leads to non-monotonous variation of PL intensity (Fig.2, black curve): the highest PL intensity was observed for the layers deposited at r_H=50-60%. At the same time, gradual decrease of lifetime was observed (Fig. 2, red curve). It should be noted that due to the high reactive ability of hydrogen, the increase of r_H has to result in the increase of excess Si content. The latter could be one of the reasons of the decrease of Er lifetime. At the same time the decrease of Er lifetime with the increasing of T_S allows to assume that the layer deposited at higher T_S has higher excess Si. This assumption was confirmed by XPS and SIMS investigation of the layers. It was found that the increase of the T_S from 100 °C to 200 °C leads to the increase of Si excess from 5±2 at. % to 8.5±2 at. %, respectively.

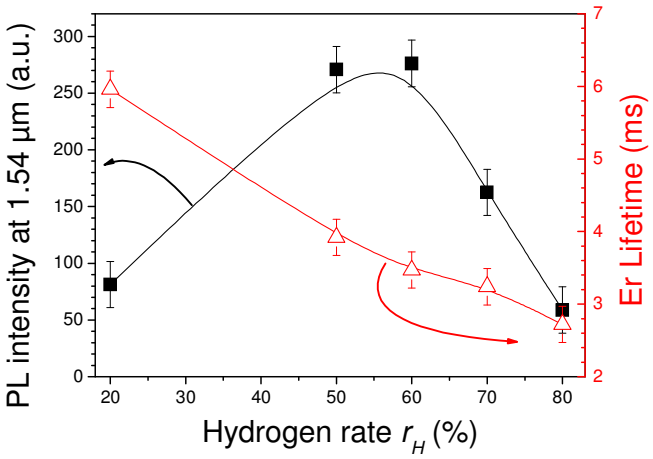

Figure 2. Dependence of Er^{3+} PL intensity (1) and lifetime (2) on the hydrogen rate, r_H. Deposition conditions: T_S=100 °C, P_{SiO2}=150 W, P_{Er2O3}=15 W. PL emission was studied under non-resonant excitation (476nm, photon flux $4x10^{18}$ ph/cm^2·s).

Based on these results, two optimized samples were fabricated at r_H =50 % and T_S=100 °C (sample A) and 200 °C (sample B). The samples have been annealed for 1 hour at 900 °C.

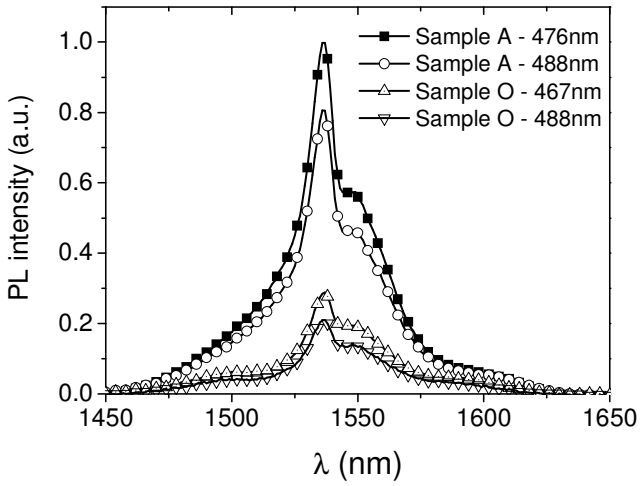

Figure 3: PL emission from the sample A and for the sample O normalised for sample thickness.

Figure 3 shows the Er^{3+} ions PL emission from sample A and sample O. The excitation has been performed both pumping resonantly with an internal erbium transition (488nm) and non-resonantly (476nm); while in the first case the erbium is excited both through direct absorption and energy transfer from Si-nc, in the latter case the ions are excited only through the Si-nc. In addition, even pumping resonantly, the erbium direct absorption is negligible with respect to the Si-nc absorption.

It is worth to note that we have been able to enhance the PL intensity by almost a factor of three for the optimized samples with respect to the sample O. Even the lifetime for the Er emission of fig. 3 showed an increase from 2 ms to almost 6 ms. No sign of cooperative up-conversion in Er ions was revealed during the lifetime measurements, pumping in a range of photon fluxes from $1x10^{16}$ to $1x10^{21}$ ph/cm^{2}s. Similar results hold for the sample B.

3. OPTICAL CHARACTERIZATION ON SLAB WAVEGUIDES

To determine the material losses of the deposited layers, Shifting Excitation Spot (SES) measurements [10] have been performed on the slab uncladded waveguides. This technique consists in exciting the sample with a micrometric pump spot on the sample surface (we used the 488 nm line of an Ar laser, resonant with an internal transition of Er ions) and shifting the spot at various distances *d* from the sample edge, where the light intensity is collected. The collection system used consists in an optical fiber coupled to a monochromator and to a liquid-nitrogen cooled InGaAs photo multiplier tube (PMT). The signal collected as a function of the distance *d* between the spot and the sample edge follows the Beer's law:

$$I(d) \propto I_0 e^{-\alpha d} \quad (1)$$

where I_0 represents the pumping spot intensity and α the losses coefficient.

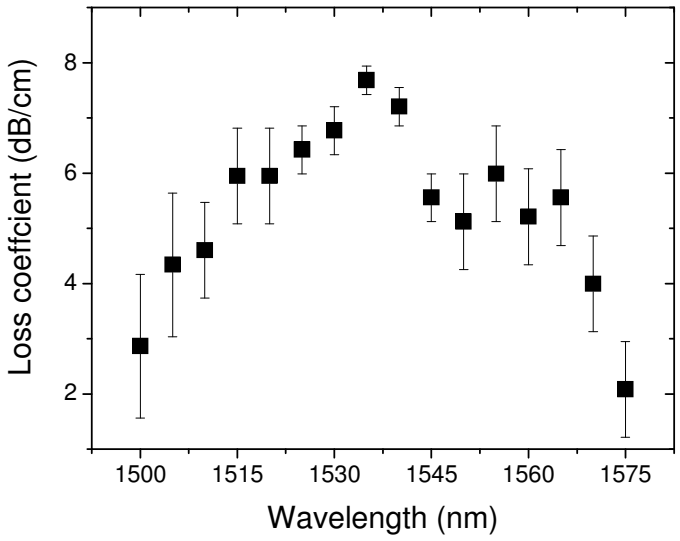

Figure 4: SES measurements pumping at 488 nm on sample A.

Figure 4 presents the results of the analysis of the SES measurements for samples A. The typical Er absorption spectrum is observed with an absorption maximum of about 8 dB/cm at about 1535 nm. At 1575 nm, where Er absorption is still present, we found material losses of about 2 dB/cm. This suggests that propagation losses are no larger than 1 dB/cm at 1610 nm where the Er absorption is negligible. Nevertheless, even if SES can give us a qualitative information, in order to obtain a reliable value of absorption coefficient it is better to perform transmission measurement in rib channel waveguide sample, as described in section (4).

It is also possible to measure the active amplification properties of the material by using the Variable Stripe Length (VSL) technique [11], which consists in pumping the slab waveguide with a narrow stripe-shaped beam, obtained by focalizing the laser beam with a cylindrical lens. Placing a blade in front of the sample it is possible to regulate the pumping stripe length L and, thus, to collect the signal as a function of this parameter. In a first approximation, the following relationship holds for the collected signal:

$$I(L) \propto \frac{1}{g}(e^{gL} - 1) \qquad (2)$$

where g is the net gain coefficient for the material.

Figure 5 summarizes the VSL results at 1540 nm for both samples as a function of the photon flux: an opposite trend is clear. Sample B shows a net decreasing g value increasing the pumping power, while sample A shows an increase of more or less 2 dB/cm for a similar photon flux increase. In the former case induced absorption is present, the latter showing internal gain (i.e. a reduction of the losses).

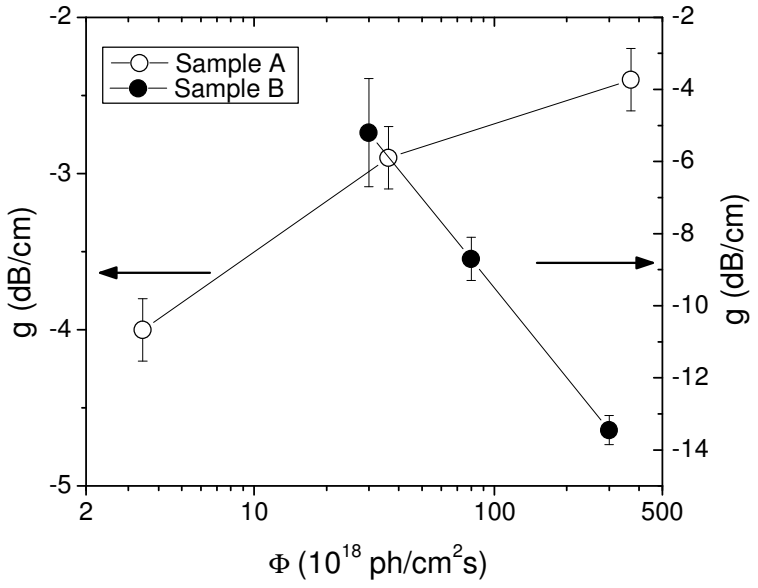

Figure 5: VSL measurements pumping at 488 nm and detecting at 1540 nm on sample A and B for three different pump photon fluxes.

We believe that in sample B the CA mechanism is dominant with respect to optical amplification and thus the material losses increase with the pump flux. In sample A, we have observed a reduction of the material losses with increasing the pump photon flux: this result hints towards a reduction of the magnitude of CA phenomenon with respect to sample B. This can be expected considering the lower Si excess of sample A. Extrapolating some quantitative results from Fig. 5, we can obtain the internal material gain. Let us considerthe *g* coefficient measured in the VSL experiment,

$$g = (2g_{int} - \alpha_{abs} - \alpha_{prop}) \rightarrow g_{int} = \frac{1}{2}(g + \alpha_{abs} + \alpha_{prop}) \quad (3)$$

where g_{int} is the internal gain, α_{abs} is the absorption loss coefficient measured from transmission spectrum in rib waveguide (see chapter 4) and α_{prop} is the propagation loss coefficient. Substituting the numerical values, we found a material internal gain of about 1 - 2 dB/cm for sample A. .

4. OPTICAL CHARACTERIZATION ON RIB WAVEGUIDES

Sample A has been chosen to define a rib waveguide structure to perform transmission and pump & probe experiments. Simulations have been performed by using a commercial, full-vectorial effective-index solver to properly design the rib waveguide.

The final etching choice was of 0.6 μm, determining a confinement factor of 0.76 for the a rib channel with width 5 μm.

After the processing, waveguide geometry has been checked performing Atomic Force Microscopy measurements (AFM). The average roughness of the sample was checked both on top and between channels leading to a result of about 5 nm. Fig. 6 reports the simulated shape of the fundamental TE-like mode together with the experimenta image taken with a CCD Infrared Camera placed at the output of the waveguide facet.

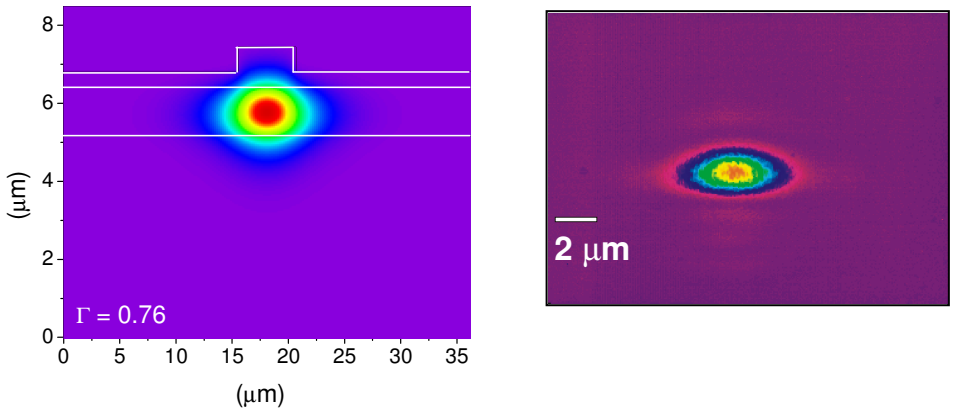

Figure 6: Simulated (left panel) and measured (right panel) field intensity for the first order TE-like mode in rib-waveguide sample A.

An average FWHM of 7 μm for the horizontal field profile for a channel width of 5 μm has been calculated and verified experimentally.

Optical losses in the rib waveguide samples have been determined by transmission measurements using a tunable infrared laser coupled to the sample through a single-mode infrared tapered optical fiber (butt coupling) and collecting the guided signal by using a 40x microscope objective. In general, the total losses inside an optical waveguide (Insertion Losses - IL) can be divided in length dependent losses, which follow the Beer's law described in (1) and lenght independent losses, like the coupling losses due to field mismatch between the fiber and the waveguide optical modes [12]. Using different waveguide lengths it is possible to distinguish between these two different kinds of losses, with a technique known as cut-back technique [13]. In fact, by taking the logarithm of eq. (1),

$$\log(I_{OUT}) = \alpha_{coupling} - \alpha_{propagation} l \qquad (4)$$

where $\alpha_{propagation}$ ($\alpha_{coupling}$) is the length dependent (independent) loss coefficient and l is the waveguide length.

Before investigating the active optical properties of Er-doped SRSO in the rib waveguide, we have characterized the losses by performing cut-back measurements. We measured 4 different sample lengths and 5 channel widths (3, 4.5, 5, 6 and 10 μm). Fig. 7 left shows a typical cut-back measurement for the 10 μm channel waveguide while Fig. 7 right shows the coupling coefficients as a function of the channel width.

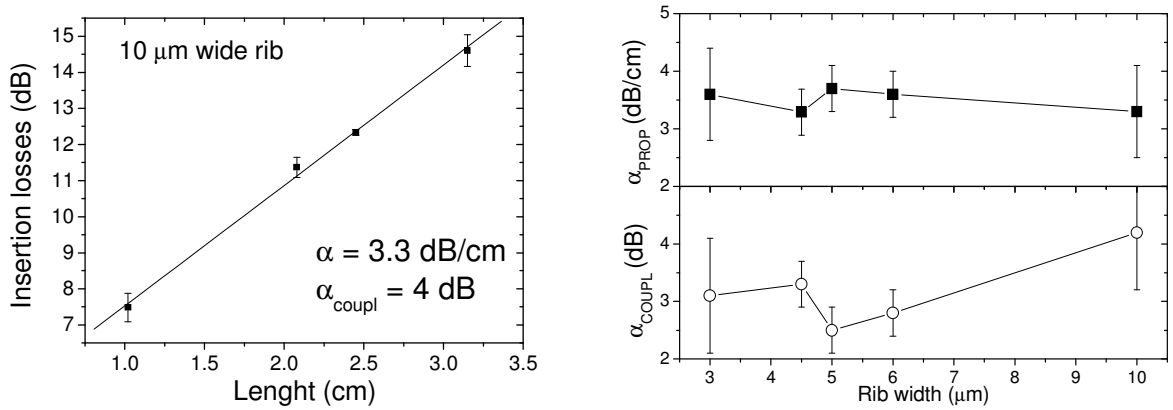

Figure 7: Cut-back results on rib waveguide sample A. Left panel: Linear fit of the insertion losses measured as a function of sample lengths. Right panel: cut-back results for different channel widths.

It is worth to note that the propagation losses measured do not depend strongly on the channel widths, and show an average value of about 3.5 dB/cm.

Fig. 8 reports the absorption spectrum for the 5 μm wide channel, after subtracting the background losses. From this result we infer an absorption loss coefficient at 1535nm of about 4 dB/cm.

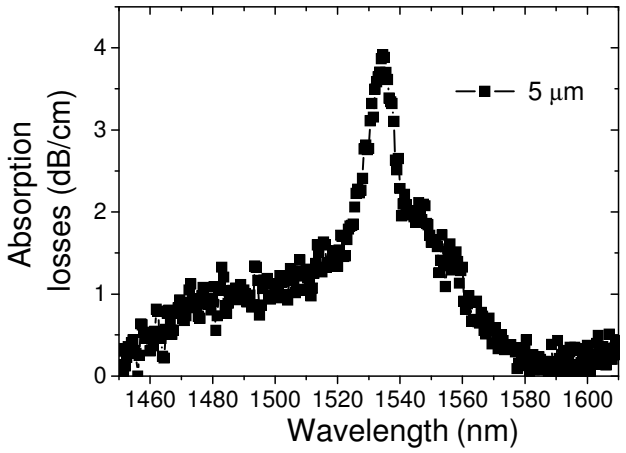

Figure 8: Absorption spectrum of the rib waveguide sample A.

At last, to investigate the active optical properties of the rib waveguide sample we have performed Pump & Probe (P&P) experiments [14] in a top-pumping scheme. The 476nm line of an Ar laser was focused in a narrow strip above a waveguide channel using a cylindrical lens while an infrared probe was butt-coupled via a tapered optical fiber into the same channel. We have used low probe power in order not to perturbe the population of the different erbium levels of the sample. Within these conditions we can obtain the Signal Enhancement (SE) factor by detecting the transmitted signal intensity in three kinds of configurations: only with the pump on the sample (I_{pump}), only with the probe on (I_{probe}) and with pump and probe on together ($I_{P\&P}$):

$$\begin{cases} I_{probe} = I_0 e^{-\alpha \Gamma L} \\ I_{pump} = I_{ASE} \\ I_{P\&P} = I_{ASE} + I_0 e^{-\alpha \Gamma L} e^{2 g_{int} \Gamma L_{pump}} \end{cases} \qquad (5)$$

where L_{pump}, L are respectively the pumped and the waveguide length, Γ is the waveguide confinement factor, I_{ASE} is the Amplified Spontaneous Emission signal and g_{int} the internal gain coefficient [15]. The SE is thus defined:

$$SE = \frac{I_{P\&P} - I_{pump}}{I_{probe}} = e^{2 g_{int} \Gamma L_{pump}} \qquad (6)$$

From the SE is straightforward to get the internal gain coefficient $\Gamma g_{int} = \frac{\ln(SE)}{2L_{pump}}$.

The measurements have been performed for two different probe wavelengths, respectively at Er^{3+} gain spectrum peak (1535nm) and almost outside the gain spectrum (1610nm). Since we are interested in the role of Si-nc as erbium sensitizers, we have excited the ions pumping non-resonant with Er^{3+} ions internal transitions (476nm). Fig. 8 reports the results.

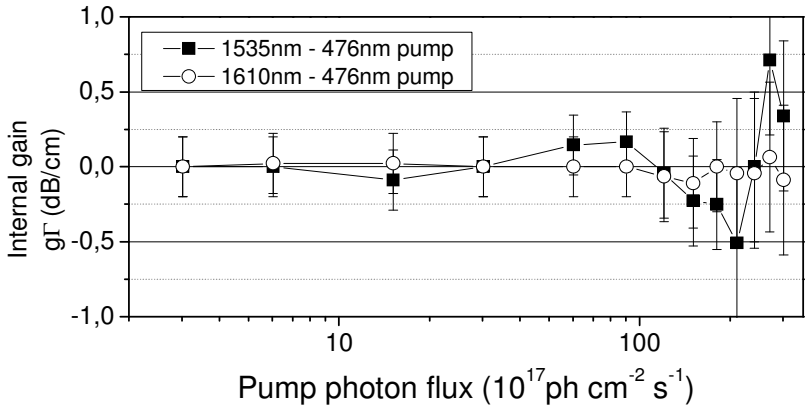

Figure 8: Pump & Probe measurements on sample A for probe wavelength of 1535 and 1600 nm. Note the logarithmic scale of the x axis.

The internal gain is zero within the error bars in a wide range of pumping fluxes (from $1x10^{16}$ to $1x10^{19}$ ph/cm^{2}s), and shows a positive value for the Er-gain peak wavelength probe (1535nm) while remaining zero for the probe wavelength outside the Er emission peak (1610nm).

Considering a confinement factor of 0.76, at medium photon fluxes, we have measured a maximum internal gain of more than 1 dB/cm. It is worth to note that thermal oscillations effects make the measurement less reliable at higher photon fluxes.

The SE for the 1610 nm probe wavelength appears to be independent from the pump photon flux, which leads us to conclude that the CA losses are negligible in this device.

Taking into account that the absorption loss at the Er peaks at 4 dB/cm, it would be possible to reach a maximum internal gain of 8 dB/cm ($2g_{int}$) by inverting all the Er population. Therefore, even considering a negligible CA in the material it is mandatory to be able to efficiently couple a larger percent of Er ions to get net optical amplification in the device. We can roughly estimate the percent of erbium coupled to Si-nc in our system ($N_{c,Sinc}$) by assuming that all the Er^{3+} coupled to Si-nc is excited and comparing the internal gain and the absorption coefficient that we measured in the rib waveguide sample. In fact, the following relationship holds:

$$\frac{\alpha_{abs}}{g_{int}} = \frac{\sigma_{abs} N_{Er}}{2\sigma_{emis} N_{c,Sinc}} \sim \frac{N_{Er}}{2N_{c,Sinc}} \rightarrow N_{c,Sinc} = \frac{g_{int}}{\alpha_{abs}} N_{Er} \quad (7)$$

Substituting the value measured in P&P and transmission experiments described in section (4.2), we found $N_{c,Sinc} \sim \frac{1}{4} N_{Er}$, that corresponds to 25 % of optically active Er ions.

5. CONCLUSIONS

In this work we have shown that we have been able to reduce CA induced losses in Er-doped SRSO samples both through an engineering of Si nanoclusters size (choosing opportune Si concentrations) and coupling a good percent of Er ions to Si-nc, the highest fraction up to date to our knowledge without back transfer issues . Nevertheless, even if reducing the CA mechanism is a necessary condition to obtain net amplification, it is not sufficient: in fact it is mandatory to understand with great care the exact nature of transfer mechanisms from nanocluster to ions and then optimize the number of efficiently coupled Er^{3+}. In this way one could hope to invert more than 50% of the Er ions.

ACKNOWLEDGMENTS

The authors would like to thank the financial support by EC through the project LANCER and in particular C.J. Oton and W. Loh (ORC, University of Southampton, UK) for the processing.

REFERENCES

1. P. C. Becker, N. A. Olson, J. R. Simpson, *Erbium-doped fiber amplifier - Fundamental and technology*, Academic Press, London, 1999.
2. J. Miniscalco, "Erbium-doped glasses for fiber amplifiers at 1500 nm", *J. Lightwave Technol.*, 9:234, 1991.
3. D. Navarro-Urrios, M. Melchiorri, N. Daldosso, L. Pavesi, C. Garcia, P. Pellegrino, B. Garrido, G. Pucker, F. Gourbilleau, R. Rizk, "Optical losses and gain in silicon-rich silica waveguides containing Er ions", *J. Lumin.*, 121:249-255, 2006.
4. D. Navarro-Urrios, A. Pitanti, N. Daldosso, F. Gourbilleau, R. Rizk, G. Pucker, L. Pavesi, "Quantification of the carrier absorption losses in Si-nanocrystal rich rib waveguides at 1.54 μm", *Appl. Phys. Lett.*, 92:051101, 2008.
5. B. Garrido, C. Garcia, P. Pellegrino, D. Navarro-Urrios, N. Daldosso, L. Pavesi, F. Gourbilleau, R. Rizk, "Distance dependent interaction as the limiting factor for Si nanocluster to Er energy tranfer in silica", *Appl. Phys. Lett.*, 89:163103, 2006.
6. I. Izeddin, A. S. Moskalenko, I. N. Yassievich, M. Fujii, T. Gregorkiewicz, "Nanosecond dynamics of the near-infrared photoluminescence of Er-doped SiO_2 sensitized with Si nanocrystals", *Phys. Rev. Lett.*, 97:207401, 2006.
7. D. K. Schroder, R. N. Thomas, J. C. Swartz, "Free carrier absorption in silicon", *IEEE T. Electron. Dev.*, ED-25:254, 1978.
8. F. Gourbilleau, C. Dufour, M. Levalois, J. Vicens, R. Rizk, C. Sada, F. Enrichi, G. Battaglin, "Room-temperature 1.54 μm photoluminescence from Er-doped Si-rich silica layers obtained by reactive magnetron sputtering", *J. Appl. Phys.*, 94:3869, 2003.
9. P. K. Tien, R. Ulrich, R. J. Martin, "Modes of propagating light waves in thin deposited semiconductor films", *Appl. Phys. Lett.*, 14:291, 1969.
10. J. Valenta, I. Pelant, J. Linnros, "Waveguide effects in the measurement of optical gain in a layer of Si nanocystals", *Appl. Phys. Lett.*, 81:1396, 2002.
11. K. L. Shaklee, R. F. Leheny, R. E. Nahory, "Stimulated emission from the excitonic molecules in CuCl", *Phys. Rev. Lett.*, 26:888, 1971.
12. R. Osellame, N. Chiodo, G. D. Valle, S. Taccheo, R. Ramponi, G. Cerullo, A. Killi, U. Morgner, M. Lederer, D. Kopf, "Optical waveguide writing with a diode-pumped femtosecond oscillator", *Opt. Lett.*, 29:1900 - 1902, 2004.
13. O. A. Vlasenko, E. M. Zolotov, R. F. Tavlykaev, "Method for measuring losses in channel waveguides", *Sov. J. Quant. Electron.*, 19:681-682, 1989.

14. D. Navarro-Urrios, N. Daldosso, C. Garcia, P. Pellegrino, B. Garrido, F. Gourbilleau, R. Rizk, L. Pavesi, “Signal Enhancement, Limiting Factors in Waveguides Containing Si Nanoclusters, Er^{3+} ions”, *Jap. J. appl. Phys.*, 46:6626, 2007.
15. B. E. A. Saleh, M. C. Teich, *Fundamentals of photonics*, John Wiley & Sons, 1991.